Effect of local strain distribution on concurrent microstructural evolution during superplastic deformation of Al–Li 8090 alloy

V. Pancholi, B.P. Kashyap *

Department of Metallurgical Engineering and Materials Science, Indian Institute of Technology, Bombay, Mumbai 400 076, India

Abstract

Superplastic deformation of Al–Li 8090 alloy was carried out to study the effect of local strain developed on the microstructural variation along the gauge length of tensile specimens. For this, separate specimens were deformed to failure at a constant temperature of 530 °C and at the strain rates within the superplastic regime. The strain distribution was found to be non-uniform with more deformation towards fracture tip and less towards the shoulder section of specimens. The grain size was found to decrease with increase in local strain whereas cavity size and cavity volume fraction were found to increase. The cavity growth in longitudinal direction is suggested to be controlled by power law but the same in transverse direction is controlled by diffusional process. A model is proposed for cavity nucleation on the basis of inhomogeneity in microstructure and its implication in deformation mechanism.

Keywords: Superplasticity; Local strain; Microstructural evolution

1. Introduction

The term superplasticity is used to define very large elongation of several hundred percent, shown by certain fine grained materials (grain size <10 μm), usually in the strain rate range of around 10^{-3}–10^{-5} s^{-1}, and at temperatures above 0.5 T_m (where T_m is absolute melting point). The stress is highly strain rate dependent in the superplastic regime, and can be expressed as $\sigma = K\dot{\varepsilon}^m$, where σ is the stress at a strain rate of $\dot{\varepsilon}$, m is strain rate sensitivity index of values $\geqslant 0.3$, and K is a material constant. The maximum ductility of superplastic material is highly sensitive to not only the initial microstructure of the material, but also to that which develops during the course of deformation. Hence, evolution of microstructure plays very important role in deciding the maximum ductility attained by the material. The evolution of microstructure during superplastic deformation reveals dynamic grain growth, dynamic recrystallization, and cavitation, etc. Dynamic grain growth and cavitation [1–3] are considered to reduce the tensile ductility of the superplastic material, whereas continuous dynamic recrystallization [4–6] is considered to be the one of the possible superplastic deformation mechanism, which can enhance ductility.

There appears [4,7–9] a lot of debate on the possible deformation mechanisms for superplasticity in Al–Li 8090 alloy, due to the sandwiched microstructure in the planes normal to rolling plane of superplastically formable sheet. In the through thickness the outer 1/3rd layers on both the sides consist of recrystallized microstructure, and the middle layer remains unrecrystallized. The initial deformation under superplastic conditions is considered to convert the low angle subgrain boundaries in the mid-section into boundaries with high misorientation angles through dislocation activity [4]. After that the deformation mechanism is considered to be grain boundary (GB) sliding [7] as common in other superplastic materials. However, Blackwell and Bate [8] argued that the dislocation motion plays important

role as a dominant mechanism through out the deformation of Al–Li 8090 alloy. This led to the study of texture evolution in this alloy. Fan et al. [9] deformed the tensile specimens machined from individual layers, representing the mid-thickness and center layers of this alloy, which showed randomization of texture in the middle layer. This suggests that the GB sliding is a dominant mechanism for superplasticity of this alloy as well once the recrystallization is complete. Like in other Al alloys [10–13], cavitation is shown to limit the maximum ductility in this alloy also. Cavities are supposed to nucleate at the interface of grain and precipitate and triple junctions, and grow through diffusion mechanism at low strains and deformation induced plasticity mechanism at high strains [14].

Superplastic flow being a non-Newtonian mechanism ($m < 1$) develops strain gradient in the gauge section from fracture tip to the section near the shoulder of the tensile sample. This strain gradient developed during deformation is expected to affect the microstructural evolution, which in turn could influence the elongation to failure. The literature available on strain gradient in the gauge section of tensile specimens during superplastic deformation only reports [15,16] the effect of strain and strain rate on local strain distribution along the gauge length. Some qualitative observations of cavity morphology were reported along the gauge of the tensile sample in Zn–22% Al alloy [17]. Recently Wang et al. [18] did a quantitative analysis on the effect of local strain on the cavitation behavior of 3Y-TZP. No such study was made in the superplastic Al–Li 8090 alloy, which has layered microstructure [8]. Therefore, the aim of the present work is to characterize quantitatively the effect of local strain and strain rate variation on microstructural evolution (comprising of grain growth and cavitation) during superplastic deformation of Al–Li 8090 alloy.

2. Experimental

The commercial superplastic grade Al–Li 8090 alloy was obtained in the form of 1.7 mm thick sheet. The composition (wt.%) of the material was Al–2.7Li–1.4Cu–0.56Mg–0.12Zr. The samples for tensile test were machined by keeping the tensile axis parallel to the rolling direction. The sample dimensions were 10 mm gauge length and 5 mm gauge width. The tests were carried out by pin loading of 6 mm diameter on an Instron universal testing machine. The test temperature was maintained at 530 ± 1 °C in a three zone split furnace. The tests were carried out to the fracture at constant initial strain rates. The deformed samples were immediately cooled in cold water to arrest the evolved microstructure. Before tensile testing, the gauge section was divided in ten sections by scratching lines at 1 mm intervals using height gauge. The markers were scratched to find out the distribution in local strain after deformation and to examine local variation in microstructural parameters from fracture tip to the section near shoulder. The material was tested under four different conditions of: (a) in as-received condition at the initial strain rate of 3.3×10^{-3} s^{-1}, (b–d) after annealing at 540 °C for 5 min, at initial strain rates of (b) 3.4×10^{-3} s^{-1}, (c) 1.7×10^{-3} s^{-1} and (d) 8.2×10^{-4} s^{-1}.

After deformation to failure the final dimensions of each marked sections of the samples were measured in three mutually perpendicular directions viz. along gauge length, in width and thickness directions, and then the samples for metallography were cut from each sections. The samples were cut from longitudinal plane (L) and transverse plane (T) and mounted sequentially from fracture tip to the section near shoulder. The mounted samples were first polished on SiC papers going up to 1200 grid size. Then cloth polishing was carried out with magnesia. Final polishing was carried out on 0.25 μm diamond paste. Etching was done using the Keller's reagent (1.5% HCl–2.5% HNO_3–1% HF–95% H_2O). The grain size (mean intercept length) was determined in L and T planes by measuring average linear intercept in the corresponding directions viz. longitudinal (d_L) and transverse (d_T), respectively. The average cavity size was determined by measuring each cavity individually from the photomicrographs, which were taken from longitudinal plane and transverse plane of the sections previously marked. The measurements were done in the longitudinal (C_L) and transverse (C_T) directions. The number of cavities measured for averaging in each section was around 100–150. The cavity volume fraction was determined by point counting method of the grids superimposed on the photomicrographs of longitudinal and transverse sections.

3. Results

The microstructure of the as-received material could not be revealed by optical microscope. However, after annealing for just 5 min at the temperature of 540 °C, a well-etched structure as shown in Fig. 1 was produced. Due to symmetry in microstructure about mid-thickness the microstructure is shown up to mid-section in T and L planes. The microstructure consists of: (a) Li depleted layer, as seen in the top position of longitudinal and transverse sections, (b) fully recrystallized pancake shaped grains, elongated in longitudinal and transverse directions in the surface layer adjacent to Li depleted layer, and (c) elongated unrecrystallized microstructure in the middle layer. No such structural gradient was found to exist in thickness direction in both T and L planes after deformation. The representative microstruc-

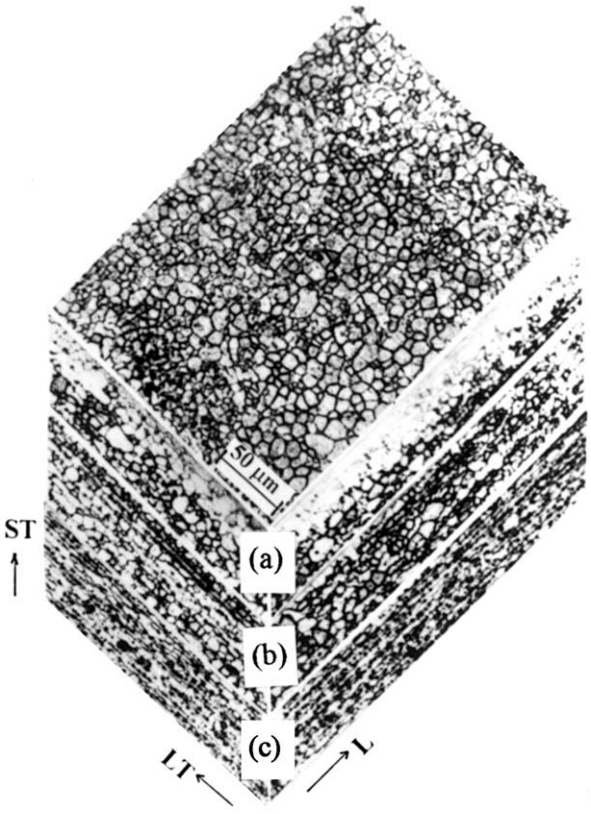

Fig. 1. 3D view of the microstructure after annealing at 540 °C for 5 min: (a) Li depleted layer, (b) layer with recrystallized microstructure and (c) middle layer of unrecrystallized grains.

tures after deformation in longitudinal and transverse sections are shown in Fig. 2. Both in the longitudinal and transverse sections the grains are fully recrystallized. Only in the section near shoulder the microstructure is not etched properly.

3.1. Variation in local strain

The local strains in various sections are plotted against the normalized distance as shown in Fig. 3, for four different conditions of deformation. The normalized distance was obtained by dividing the distance of marker from the fracture tip by the final gauge length of the sample [19]. While the strain in the vicinity of fracture tip is noted to be large ($\sim$ 300–500%) the same decreases, to much lower values ($\sim$ 50–200%) near the shoulder of tensile specimens.

3.2. Grain size variation

The average grain sizes obtained in different regions of the tensile specimens are plotted against local strain in Fig. 4(a)–(d). It is apparent that d_L (grain size in longitudinal direction) is greater than d_T (grain size in transverse direction) at all the conditions of deformation and at each of the local strains. The initial microstructure also showed more grain elongation in L direction than in T direction. It is seen that the grain size decreases in both the directions with increase in local strain, from the section near the shoulder towards fracture tip. It is found out that the variation in grain size with local strain is generally larger for the samples tested at higher strain rates, Fig. 4(a), (b), than that at lower strain rates, Fig. 4(c), (d). Also, the samples deformed after annealing are seen to lead systematic grain size variation as a function of local strain, whereas the sample tested in as-received condition exhibits somewhat less definite trend with a large scatter in grain size.

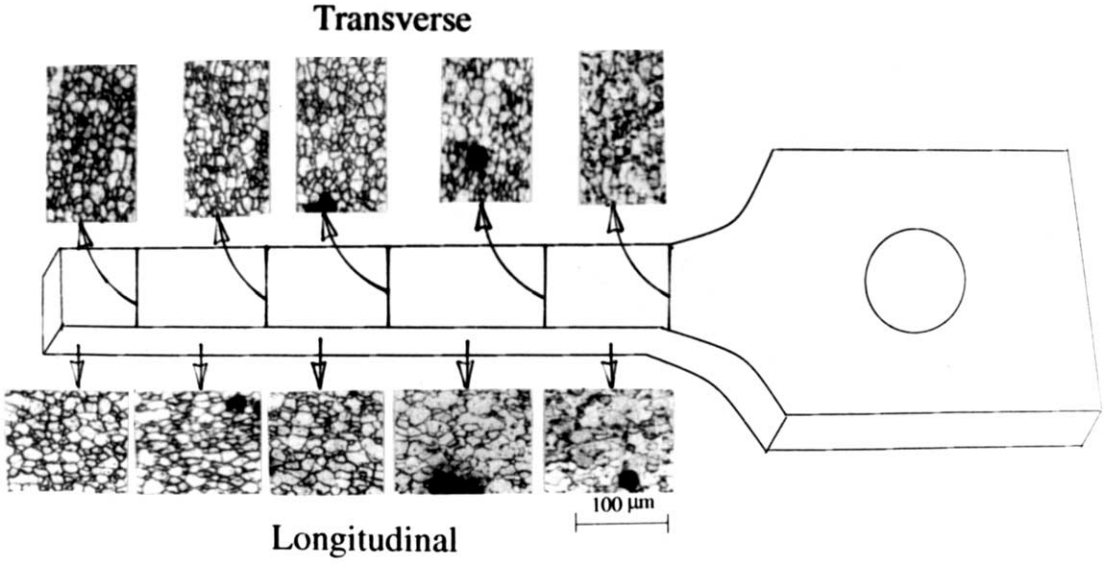

Fig. 2. The representative microstructure in longitudinal and transverse sections through out one part of the gauge length after deformation to fracture.

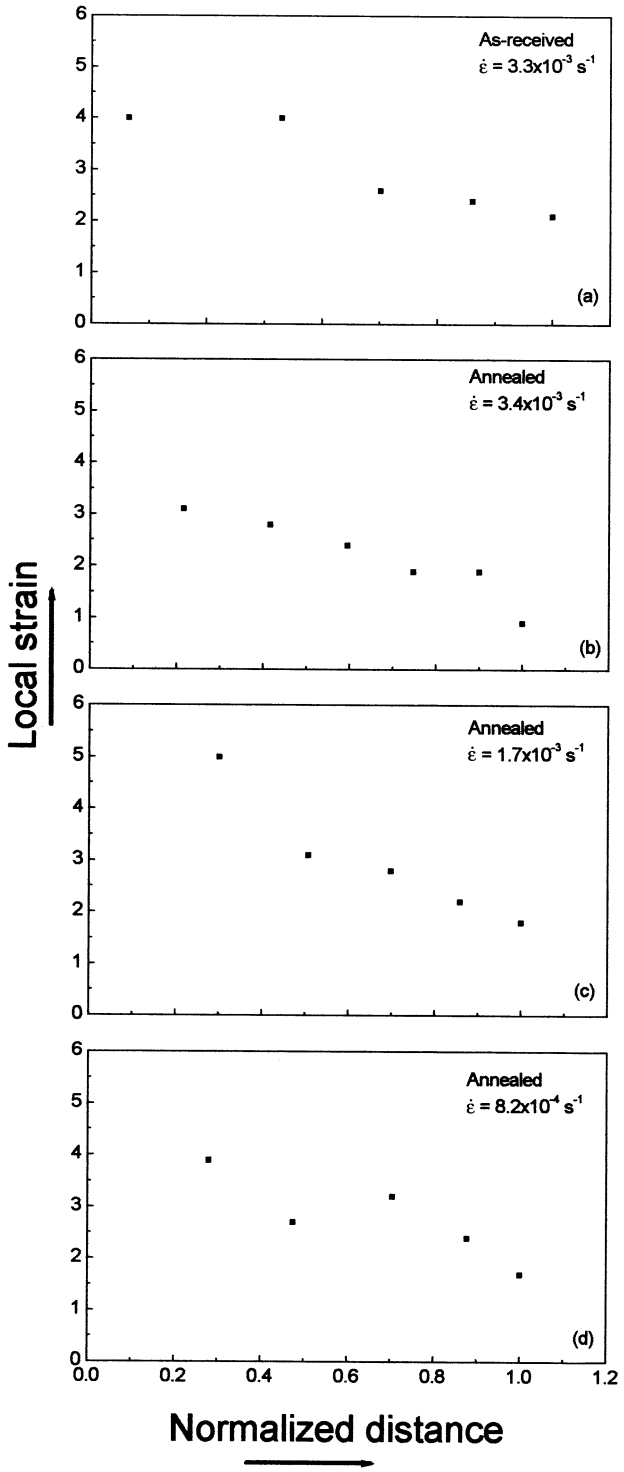

Fig. 3. Local strain ($\Delta l_i/l_i$) plotted against the normalized distance: (a) the specimen in as-received condition deformed at the initial strain rate of 3.3×10^{-3} s^{-1}; (b–d) deformed after annealing at 540 °C for 5 min, at initial strain rates of: (b) 3.4×10^{-3} s^{-1}, (c) 1.7×10^{-3} s^{-1}, (d) 8.2×10^{-4} s^{-1}.

3.3. Cavitation

The average cavity size measured in different sections is seen to increase with local strain as shown in Fig. 5(a)–(d). Whereas the sample tested in as-received condition shows a marginal increase in cavity size, the material tested after annealing is found to exhibit substantial increase in cavity size with increasing local strain. Under all test conditions, the cavity size C_T in the transverse section is found to be greater than C_L in the longitudinal section at smaller strains but a reversal in trend is suggested at larger local strains. In the pre-annealed material, tested at higher strain rates of 3.4×10^{-3} s^{-1} (Fig. 5b) and 1.7×10^{-3} s^{-1} (Fig. 5c), the cavity size is varying almost exponentially with local

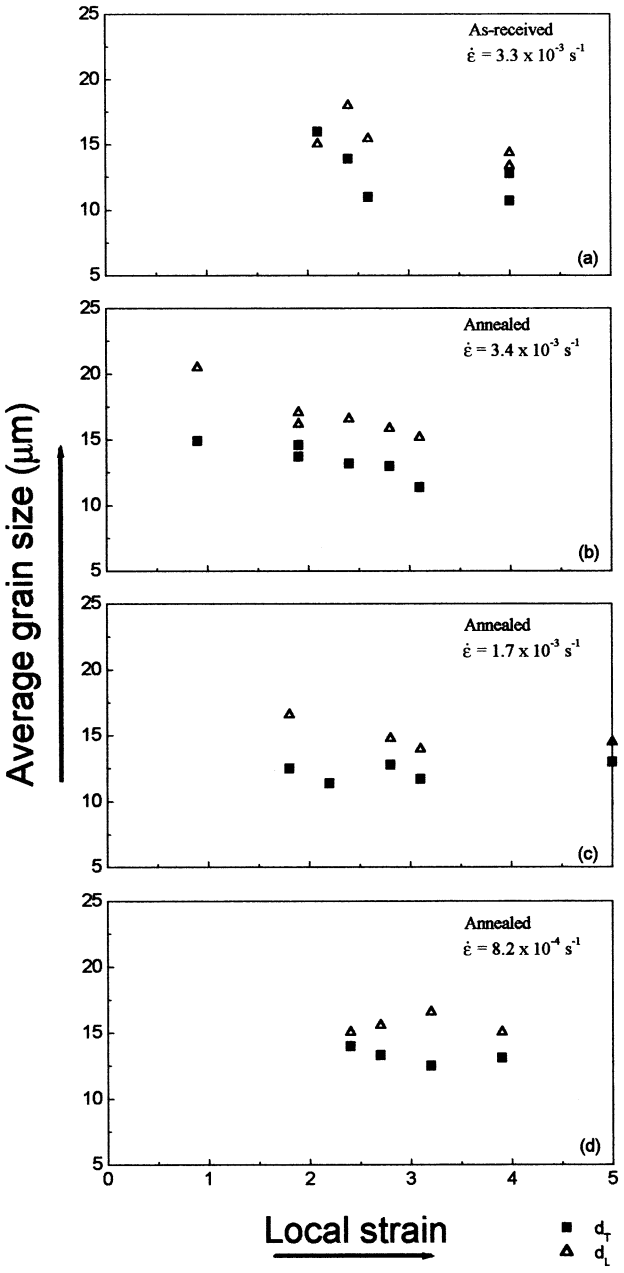

Fig. 4. Plot of average grain size vs local strain: (a) in as-received condition at the initial strain rate of 3.3×10^{-3} s^{-1}; (b–d) after annealing at 540 °C for 5 min and deformed at initial strain rates of (b) 3.4×10^{-3} s^{-1}, (c) 1.7×10^{-3} s^{-1}, (d) 8.2×10^{-4} s^{-1}.

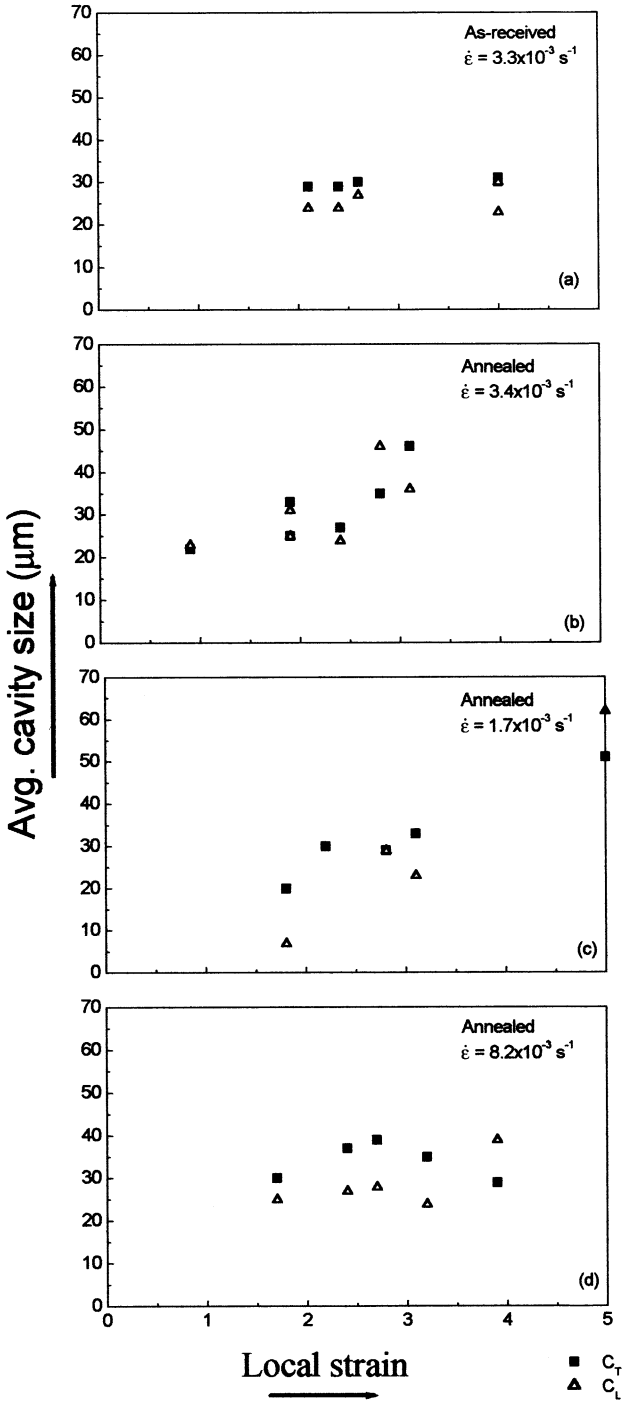

Fig. 5. Plot of average cavity size as a function of local strain: (a) in as-received condition at the initial strain rate of 3.3×10^{-3} s^{-1}; (b–d) after annealing at 540 °C for 5 min and deformed at initial strain rates of (b) 3.4×10^{-3} s^{-1}, (c) 1.7×10^{-3} s^{-1}, (d) 8.2×10^{-4} s^{-1}.

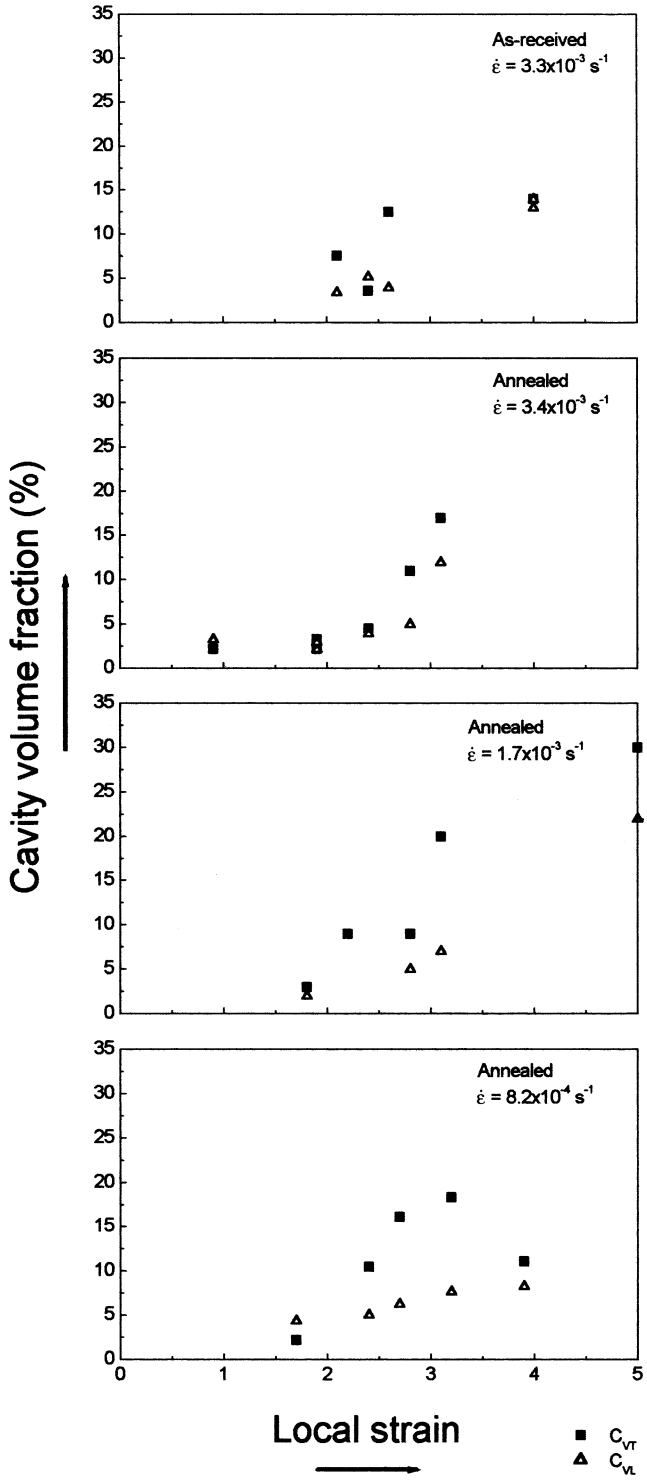

Fig. 6. Cavity volume fraction plotted against local strain: (a) in as-received condition at the initial strain rate of 3.3×10^{-3} s^{-1}; (b–d) after annealing at 540 °C for 5 min and deformed at initial strain rates of (b) 3.4×10^{-3} s^{-1}, (c) 1.7×10^{-3} s^{-1}, (d) 8.2×10^{-4} s^{-1}.

strain, whereas at low strain rate of 8.2×10^{-4} s^{-1} (Fig. 5d) the increase in cavity size is not much.

The percentage cavity volume fractions measured in transverse (C_{VT}) and longitudinal (C_{VL}) planes are plotted against local strain in Fig. 6(a)–(d). The volume fraction of cavities is not found to be more than 20% at the largest local strain (Fig. 6a, b, d), except for the pre-annealed sample tested at 1.7×10^{-3} s^{-1} (Fig. 6c), where it is closer to 35% in the transverse plane. Again, there appears scatter in the data for the sample tested in

as-received condition, whereas the samples tested after annealing show a definite trend of an increase in the volume fraction with local strain. It is also noticeable here that the volume fraction of cavities is generally more in transverse plane than in longitudinal plane in all the regions of varying local strains.

4. Discussion

4.1. Strain localization

The high elongation to failure during superplastic deformation is achieved because of resistance to necking by high strain rate sensitivity index [1]. Despite the high strain rate sensitivity index, reported to be 0.5 [7], strain localization was found in the present alloy. To understand it better, the local strain (LS) was normalized by total strain (ES), and the same (LS/ES) is plotted against normalized distance in Fig. 7. Normalizing the local strain by total engineering strain clearly indicates the non-uniformity in deformation. It may be noted that the data presented here are based on the measurements made on one part of the gauge section undergone fracture into two pieces. For superplastic material with m approaching unity, one should expect the ratio of local strain to total strain to be equal to 1 at every point along the gauge length. However, the value of strain rate sensitivity index is less than 1 in this material and hence the deviation from the ratio of 1 could be noted. As reported in the literature for other materials [15,18], in the initial stages of deformation the strain remains uniform through out the gauge. However, the strain localization is reported to take place somewhere in the middle portion of the gauge length on subjecting to large strains. A possible reason for this is that the material may be flowing from the shoulder section into the gauge section adjacent to shoulder, as some degree of curvature is often noticed in the scratch marks there. Hence, initially the strain may be uniform but eventually strain localization takes place away from the shoulder section. The occurrence of the ratio of LS/ES > 1 is due to flow localization and presence of cavities at large local strains i.e. near fracture tip. The ratio of LS/ES < 1 near the shoulder section can be attributed to the constraint imposed by the shoulder to the deforming gauge as well as to the flow of material from shoulder itself.

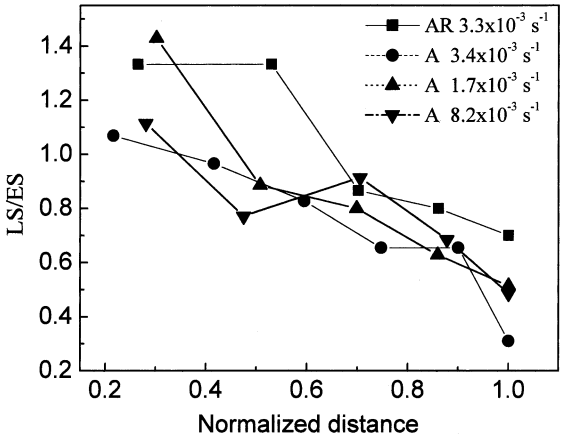

Fig. 7. Plot of ratio of local strain to total engineering strain (LS/ES) as a function of normalized distance (AR stands for as-received and A for annealed samples before test).

4.2. Microstructural variation

The unrecrystallized grains in the mid-thickness of the sample were found to have evolved into well recrystallized grains during deformation. As no microstructural gradient was noticed in through thickness direction at any location, it is apparent that the strain for the evolution of grain structure to fully recrystallized grains is less than the local strain found in all the samples. The dynamic recrystallization (DRX) during early part of the deformation in mid-thickness is through deformation induced continuous recrystallization [4], which is different from the dynamic recrystallization of nucleation and growth type.

Dynamic grain growth and grain refinement through dynamic recrystallization are well documented during superplastic deformation. Seindensticker and Mayo [20] suggested that the grain growth is the integral part of superplastic deformation. Generally, the reported data in literature are concerned only with the effect of imposed strain and strain rate on microstructure at the fracture tip. It is interesting to find here that a large extent of microstructural variation took place in a single sample along the gauge length. Though the imposed strain rate is initially same for the whole sample, subsequently the strain in each section becomes different. As the overall time for deformation remains the same for all the sections, the strain rate experienced by different section would vary as shown in Fig. 8, towards the end of deformation. The strain rate would be more in the section near the fracture region (as local strain is found to be highest there) than the section near the shoulder. The fine grains observed in the section near fracture tip may be due to dynamic recrystallization (not deformation induced continuous dynamic recrystallization) because of a high local strain rate, whereas in other sections, because of low local strain rates, grain growth could take place. Probably, this is the reason that the grain size is found to be greater in the sections near the shoulder (Fig. 4). However, such a gradient in grain size is noted only for the sample tested at the highest strain rates of 3.4×10^{-3} s^{-1}. At the low strain rate of 8.2×10^{-4} s^{-1}, the variation in grain size against local strain was not found to be much significant; the evidence suggests the occurrence of only dynamic grain growth with uniform grain size. It seems that, with increase in

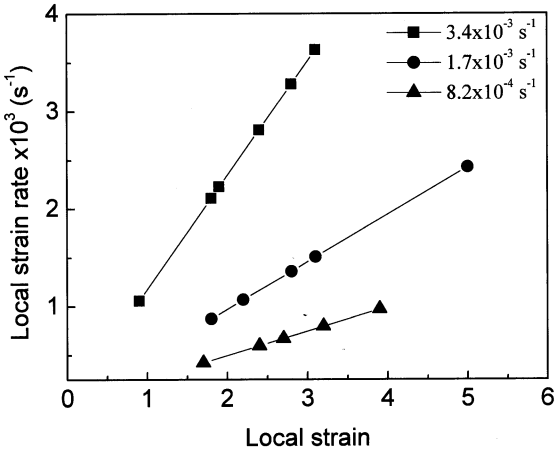

Fig. 8. Variation of local strain rate (calculated on the basis of strain rate and time elapsed in testing) with strain rate for the samples tested after annealing.

local strain rate, first dynamic grain growth tends to dominate the microstructural evolution and, only after attaining some critical strain rate (local strain rate of 2.8×10^{-3} s^{-1} or more), dynamic recrystallization becomes responsible for grain refinement. It is interesting to note here that grain sizes at the fracture tips in all the samples tested are more or less comparable. So it can be misleading to correlate the microstructural condition at the fracture tip alone.

The increase in cavity size and cavity volume fraction with local strain confirms the strain dependence of cavity growth [21]. It is surprising to note that there is no increase in cavity size and cavity volume fraction with increase in both local strain and strain rate for the material tested in as-received condition at the initial strain rate of 3.3×10^{-3} s^{-1}. It seems that initial microstructure plays important role in subsequent evolution, even after a few hundred percent of deformation. The cavity growth mechanism has a strong dependence on cavity size and strain rate of deformation. While the small cavity size and low strain rate favor diffusional growth, the large cavity size and high strain rate favor power law growth [21,22]. The appearance of cavity also changes with the type of growth process, from rounded morphology during diffusional process to elongated morphology during power law growth [23]. At lower local strains and strain rates in the vicinity of shoulder the cavity growth kinetics is controlled by diffusion of vacancies, as stresses are low there because of greater cross-sectional area and lower local strain rates. But growth of cavities would be greater in transverse direction than longitudinal direction as the concentration of vacancy is more in the boundaries transverse to the applied stress [2]. This explains the greater cavity size in transverse direction than that in longitudinal direction and also the rounded cavity morphology in both the sections, at smaller local strains. At larger local strains, the stresses in longitudinal direction can be quite high by virtue of small cross-sectional area (stress = load/area) and higher local strain rates ($\sigma \propto \dot{\varepsilon}^m$). Therefore, the large cavity size with elongated morphology was observed (Fig. 9a) due to power law growth whereas, in transverse direction, the cavity growth is still diffusion controlled, as no stresses are acting in that direction and hence cavities are rounded as shown in Fig. 9b.

4.3. Interrelationship between grain growth and cavitation

It is known that cavitation during superplastic deformation occurs more readily in relatively coarse grained materials vis-à-vis fine grained materials. Therefore, the cavitation during superplastic deformation is expected to be enhanced by the increase in grain size due to dynamic grain growth. But, the grain size referred is the average grain size without alluding to the inhomogeneity in microstructure like grain size distribution or spatial distribution. The deformation mechanism in superplasticity is considered to be GB sliding, which is very sensitive to grain size. During superplastic deformation the grain size increases with strain, which can make GB sliding and grain rotation more difficult and as such it can result in stress concentration at triple points and GB ledges [24]. As reported by Kobayashi et al. [25], the nature of GBs meeting at triple junctions also has profound impact on cavity nucleation in this material. The triple junctions connected with random boundaries and mixed GBs (CSL and random) were shown to be more probable site for cavity nucleation than the triple point connected with only special boundaries. The other possible cavity nucleation site is the interface of GB precipitates. In the Al–Li alloys of similar compositions, the cavities were shown to nucleate at the interface of the large silicon reach particles [26], and Al–Fe–Cu particles [27]. The imposed strain rate also affects the possible location of nucleation site. At high strain rates cavitation is restricted near the fracture tip, whereas at low strain rate the cavitation is uniformly distributed over the gauge length [27]. Although it may appear that the GB precipitates are the major source of cavitation, it was reported by Chokshi [28] that the reduction in grain size reduces the possibility of a cavity nucleation by relaxing stress concentration at the interface through GB diffusion.

The strain rate has a distinct effect on not only the flow stress but also on the deformation induced microstructural evolution [2,29]. The strain rate gradient developed due to the local variation in strain along the gauge length of a tensile sample introduces strain rate gradient as well, Fig. 8. Although it would be interesting to follow the effect of strain rate gradient, on grain growth/recrystallization and cavitation by conducting

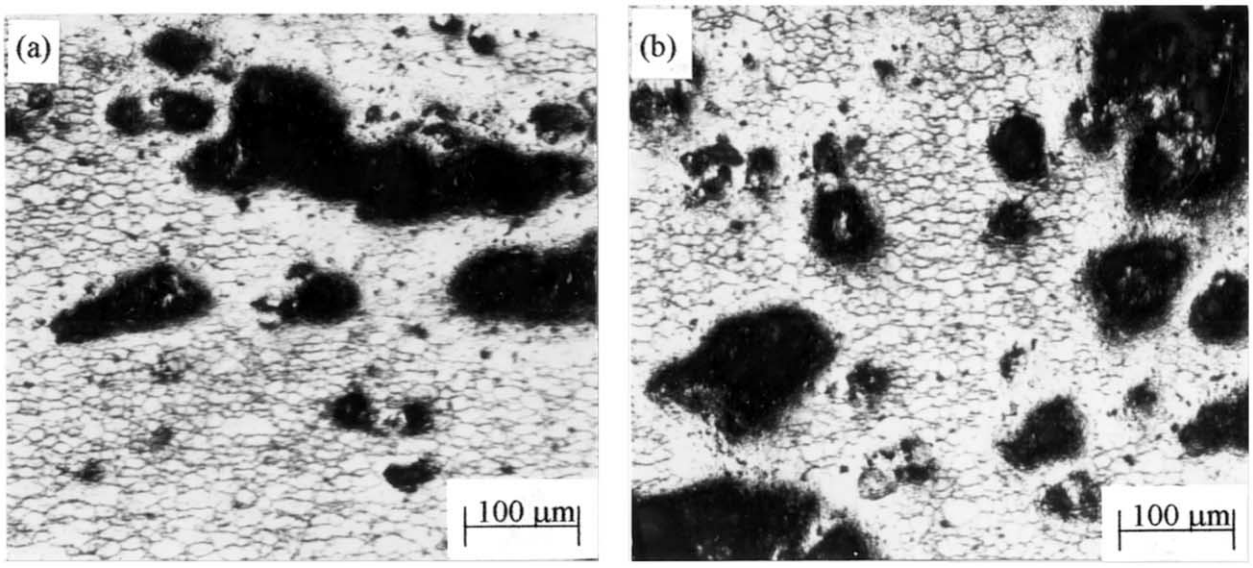

Fig. 9. Micrographs of the deformed specimen taken near the fracture tip: (a) longitudinal, (b) transverse sections.

interrupted tests to selected strain levels, only a tentative understanding can be drawn from the present work. The increase in strain rate necessitates a higher flow stress. Accordingly, the region adjoining the fracture tip (before fracture), which is deforming apparently at higher strain rates, would resist deformation due to the higher stress required. Since the necking was less diffused in the deformed specimen, it appears that the neck once formed maintained the region of maximum local strain and strain rate. The appearance of recrystallized grains near the fracture tip (Fig. 2) is thus ascribed to the development of local higher strain rates and larger strains. The local higher strain rates can facilitate nucleation of cavities, as the critical cavity size capable of growing decreases with increasing flow stress. However, the same stress can lead to grain refinement in which case the possibility of further cavity nucleation will decrease. On the other hand, the cavity growth rate may increase at lower strain rates [28] as more GBs are available for diffusion, due to grain refinement. In the present work, it is observed that even though the cavity size and volume fraction increase while going from section near the shoulder to fracture tip the grain size is found to be smaller near the fracture region than that in the sections away from fracture tip. This suggests that, instead of average grain size the local microstructural inhomogeneity plays major role in cavitation. Al–Li 8090 is reported to have a bimodal distribution of grain size i.e. cluster of coarse grains are present with the network of fine grains [30]. It is indeed found as shown in Fig. 10 that the cavities are generally surrounded by coarse grains. If we consider the model given by Ghosh and Raj [31] for superplastic deformation, where the coarse grains deform by dislocation creep and fine grains by GB sliding, the above observation can be explained. During deformation of Al–Li 8090 alloy the fine grains slide relative to each other, and cluster of coarse grains deform by dislocation creep [30]. The cluster of coarse grains has to take part in the deformation to maintain iso-strain condition, and hence the dislocation generated would be accumulating at the triple points and GBs, which can give rise to stress concentration. Now, owing to the large size of coarse grains, the stress concentration at GBs and triple points can not be relieved through grain rotation or further grain growth. When the stress concentration is sufficiently greater than the free surface energy, the cavity would nucleate [23]. Hence, instead of correlating the global average grain size with cavitation, actually these local clusters of coarse grains should be considered for

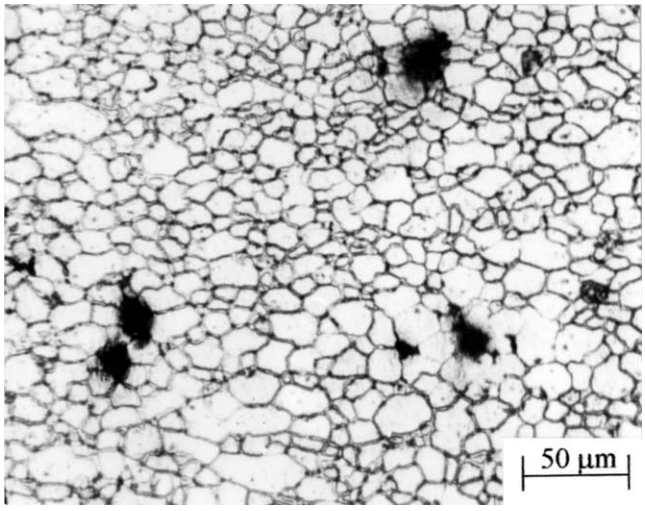

Fig. 10. Optical micrograph illustrating the presence of cavities within the cluster of coarse grains in the bi-modal grain size distribution.

cavity nucleation. However, the stress concentration due to dislocation accumulation at the interfaces between the fine grains and coarse grains can still be relieved through grain rotation and grain growth of the fine grains. Hence the interface between the fine and coarse grains which is suggested as a possible site for cavity nucleation [32] does not appear to be true in the present material. It may be possible here that the stress relaxation process still remains active in the fine grain region of the bimodal structure to avoid cavitation.

5. Conclusions

(1) The deformation is found to be non-uniform through out the gauge length. The local strain is highest near the fracture tip and lowest near the shoulder section. The variation in local strain is attributed to the value of m being less than unity as well as to the flow of some material from shoulder towards gauge during superplastic deformation.

(2) The grain size decreases with the increase in local strain. The decrease in grain size is attributed to continuous dynamic recrystallization (nucleation and growth) though the strain rates involved during superplastic deformation are an order of magnitude lower than the strain rates responsible for such recrystallization.

(3) The average cavity size and cavity volume fraction increase with the increase in local strain. The cavity growth occurs by diffusional process at smaller local strain levels in both longitudinal and transverse directions. At large local strains, cavity growth in the longitudinal direction occurs by power law growth whereas in the transverse direction cavity growth still occurs by diffusional process.

(4) Within the bi-modal distributions of grains in the present material, the cavities are found to nucleate and grow at the junction of coarse grains, and no significant cavitation is noted between the clusters of finer grains.

References

[1] T.G. Langdon, Met. Sci. 16 (1982) 175.
[2] B.P. Kashyap, A.K. Mukherjee, Res. Mechanica 17 (1986) 293.
[3] X. Jiang, J.C. Earthman, F.A. Mohamed, J. Mater. Sci. 29 (1994) 5499.
[4] L. Quing, H. Xiaoxu, Y. Mei, Y. Jinfeng, Acta Metall. Mater. 40 (1992) 1753.
[5] Y.S. Han, S.H. Hong, Mater. Sci. Eng. A266 (1999) 276.
[6] Y. Maehara, Y. Ohmori, Metall. Trans. A 18A (1987) 663.
[7] H.P. Pu, F.C. Liu, J.C. Huang, Metall. Mater. Trans. A 26A (1995) 1153.
[8] P.L. Blackwell, P.S. Bate, Metall. Trans. A 24A (1993) 1085.
[9] W. Fan, B.P. Kashyap, M.C. Chaturvedi, Mater. Sci. Technol. 17 (2001) 439.
[10] C.L. Chen, M.J. Tan, Mater. Sci. Eng. A298 (2001) 235.
[11] L.P. Troeger, E.A. Starke, Jr., Mater. Sci. Eng. A277 (2000) 102.
[12] D.H. Shin, K.T. Park, Mater. Sci. Eng. A268 (1999) 55.
[13] K. Kannan, C.H. Hamilton, Scr. Metall. 38 (1997) 299.
[14] L. Quing, H. Xiaoxu, Y. Jenfeng, Y. Mei, Scr. Metall. Mater. 25 (1991) 387.
[15] F.A. Mohamed, T.G. Langdon, Acta Metall. 29 (1981) 911.
[16] R.K. Mahidhara, Scr. Metall. Mater. 32 (1995) 1483.
[17] A.H. Chokshi, T.G. Langdon, Acta Mater. 37 (1989) 715.
[18] Z.C. Wang, N. Ridley, T.J. Davies, J. Mater. Sci. 34 (1999) 2695.
[19] M. Sagradi, D.P. Sagradia, R.E. Medrano, Acta Mater. 46 (1998) 3857.
[20] J.R. Seindensticker, M.J. Mayo, Scr. Metall. 38 (1998) 1091.
[21] D.A. Miller, T.G. Langdon, Scr. Metall. 14 (1980) 179.
[22] S.-A. Shei, T.G. Langdon, J. Mater. Sci. 13 (1978) 1084.
[23] J.W. Hancock, Met. Sci. 10 (1976) 319.
[24] A.K. Mukherjee, Superplasticity in metals, ceramics and intermetallics, in: Plastic Deformation and Fracture of Materials, H. Mughrabi (Vol. Ed.), Materials Science and Technology, A Comprehensive Treatment, Vol. 6, R.W. Cahn, P. Haasen, E.J. Kramer (Eds.), VCH Verlagsgesellschaft GmbH, D-6940 Weinheim, 1993, pp. 407–460.
[25] S. Kobayashi, T. Yoshimura, S. Tsurekawa, T. Watanabe, Mater. Sci. Forum 304–306 (1999) 591.
[26] M.C. Pandey, J. Wadsworth, A.K. Mukherjee, J. Mater. Sci. 23 (1988) 3509.
[27] A.H. Chokshi, A.K. Mukherjee, Mater. Sci. Eng. A110 (1989) 49.
[28] A.H. Chokshi, Mater. Sci. Forum 233–234 (1997) 89.
[29] B.P. Kashyap, A. Arieli, A.K. Mukherjee, J. Mater. Sci. 20 (1985) 2661.
[30] A.H. Chokshi, A.K. Mukherjee, Metall. Trans. A 19A (1988) 1621.
[31] A.K. Ghosh, R. Raj, Acta Metall. 34 (1986) 447.
[32] A. Bussiba, A.B. Artzy, A. Shtechman, S. Ifergan, M. Kupiec, Mater. Sci. Eng. A302 (2001) 56.